
1 **Attribution of growing season evapotranspiration variability**
2 **considering snowmelt and vegetation changes in the arid alpine**
3 **basins**

4 Tingting Ning^{abc*}, Zhi Li^d, Qi Feng^{ac*}, Zongxing Li^{ac} and Yanyan Qin^b

5 *^aKey Laboratory of Ecohydrology of Inland River Basin, Northwest Institute of Eco-Environment and Resources,*

6 *Chinese Academy of Sciences, Lanzhou, 730000, China*

7 *^bKey Laboratory of Land Surface Process and Climate Change in Cold and Arid Regions, Chinese Academy of*

8 *Sciences, Lanzhou 730000, China*

9 *^cQilian Mountains Eco-environment Research Center in Gansu Province, Lanzhou, 730000, China*

10 *^dCollege of Natural Resources and Environment, Northwest A&F University, Yangling, Shaanxi, 712100, China*

11 * Correspondence to: Qi Feng (qifeng@lzb.ac.cn)

12

13 **Abstract:** Previous studies have successfully applied variance decomposition
14 frameworks based on the Budyko equations to determine the relative contribution of
15 variability in precipitation, potential evapotranspiration (E_0), and total water storage
16 changes (ΔS) to evapotranspiration variance (σ_{ET}^2) on different time-scales; however,
17 the effects of snowmelt (Q_m) and vegetation (M) changes have not been incorporated
18 into this framework in snow-dependent basins. Taking the arid alpine basins in the
19 Qilian Mountains in northwest China as the study area, we extended the Budyko
20 framework to decompose the growing season σ_{ET}^2 into the temporal variance and
21 covariance of rainfall (R), E_0 , ΔS , Q_m , and M . The results indicate that the
22 incorporation of Q_m could improve the performance of the Budyko framework on a
23 monthly scale; σ_{ET}^2 was primarily controlled by the R variance with a mean
24 contribution of 63%, followed by the coupled R and M (24.3%) and then the coupled
25 R and E_0 (14.1%). The effects of M variance or Q_m variance cannot be ignored
26 because they contribute to 4.3% and 1.8% of σ_{ET}^2 , respectively. By contrast, the
27 interaction of some coupled factors adversely affected σ_{ET}^2 , and the ‘out-of-phase’
28 seasonality between R and Q_m had the largest effect (-7.6%). Our methodology and
29 these findings are helpful for quantitatively assessing and understanding hydrological
30 responses to climate and vegetation changes in snow-dependent regions on a finer
31 time-scale.

32 **Keywords:** evapotranspiration variability; snowmelt; vegetation; attribution

33 **1 Introduction**

34 Actual evapotranspiration (ET) drives energy and water exchanges among the
35 hydrosphere, atmosphere, and biosphere (Wang et al., 2007). The temporal variability
36 in ET is, thus, the combined effect of multiple factors interacting across the
37 soil–vegetation–atmosphere interface (Katul et al., 2012; Xu and Singh, 2005).
38 Investigating the mechanism behind ET variability is also fundamental for
39 understanding hydrological processes. The basin-scale ET variability has been widely
40 investigated with the Budyko framework (Budyko, 1961, 1974); however, most
41 studies are conducted on long-term or inter-annual scales and cannot interpret the
42 short-term ET variability (e.g. monthly scales).

43 Short-term ET and runoff (Q_r) variance have been investigated recently for their
44 dominant driving factors (Feng et al., 2020; Liu et al., 2019; Wu et al., 2017; Ye et al.,
45 2015; Zeng and Cai, 2015; Zeng and Cai, 2016; Zhang et al., 2016a); to this end, an
46 overall framework was presented by Zeng and Cai (2015) and Liu et al. (2019). Zeng
47 and Cai (2015) decomposed the intra-annual ET variance into the variance/covariance
48 of precipitation (P), potential evapotranspiration (E_0), and water storage change (ΔS)
49 under the Budyko framework based on the work of Koster and Suarez (1999).
50 Subsequently, Liu et al. (2019) proposed a new framework to identify the driving
51 factors of global Q_r variance by considering the temporal variance of P , E_0 , ΔS , and
52 other factors such as the climate seasonality, land cover, and human impact. Although

53 the proposed framework performs well for the ET variance decomposition, further
54 research is necessary for considering additional driving factors and for studying
55 regions with unique hydrological processes.

56 The impact of vegetation change should first be fully considered when studying the
57 variability of ET . Vegetation change significantly affects the hydrological cycle
58 through rainfall interception, evapotranspiration, and infiltration (Rodriguez-Iturbe,
59 2000; Zhang et al., 2016b). Higher vegetation coverage increases ET ~~but and~~ reduces
60 the ratio of Q_r to P (Feng et al., 2016). However, most of the existing studies on ET
61 variance decomposition either ignored the effects of vegetation change or did not
62 quantify its contributions. Vegetation change is closely related to the Budyko
63 controlling parameters, and several empirical relationships have been successfully
64 developed on long-term and inter-annual scales (Li et al., 2013; Liu et al., 2018;
65 Ning et al., 2020; Xu et al., 2013; Yang et al., 2009). However, the relationship
66 between vegetation and its controlling parameters on a finer time-scale has received
67 less attention. As such, it is important to quantitatively investigate the contribution of
68 vegetation change to ET variability on a finer time-scale.

69 Second, for snow-dependent regions, the short-term water balance equation was the
70 foundation of decomposing ET /or Q_r variance. Its general form can be expressed
71 as:the water balance equation should be modified to consider the influence of
72 snowmelt in short-term time scale, which has been the foundation for decomposing

73 ~~ET or runoff variance and is expressed as:~~

$$74 \quad P = ET + Q_r + \Delta S, \quad (1)$$

75 where P , including liquid (rainfall) and solid (snowfall) precipitation, is the total water
76 source of the hydrological cycle. ~~However,~~But this equation is unsuitable for regions
77 where the land-surface hydrology is highly dependent on the winter mountain
78 snowpack and spring snowmelt runoff. ~~It has been reported that The global~~ annual Q_r
79 originating from snowmelt accounts for 20–70% of the total runoff, including west
80 United States (Huning and AghaKouchak, 2018), coastal areas of Europe (Barnett et
81 al., 2005), west China (Li et al., 2019b), northwest India (Maurya et al., 2018), south
82 of the Hindu Kush (Ragettli et al., 2015), and high-mountain Asia (Qin et al., 2020).

83 In these regions, the mountain snowpack serves as a natural reservoir that stores
84 cold-season P to meet the warm-season water demand (Qin et al., 2020; Stewart,
85 2009). Thus, the water balance equation should be modified to consider the impacts of
86 snowmelt on runoff in short-term time scale~~As such, the water balance equation in~~
87 ~~these regions on a short time scale should be rewritten as:~~

$$88 \quad R + Q_{sm} = ET + Q_r + \Delta S, \quad (2)$$

89 where R is the rainfall, and Q_{sm} is the snowmelt runoff. Many observations and
90 modelling experiments have found that due to global warming, increasing
91 temperatures would induce earlier runoff in the spring or winter and reduce the flows

92 in summer and autumn (Barnett et al., 2005; Godsey et al., 2014; Stewart et al., 2005;
93 Zhang et al., 2015). Therefore, the role of snowmelt change on *ET* variability in
94 snow-dependent basins on a finer time-scale should be studied.

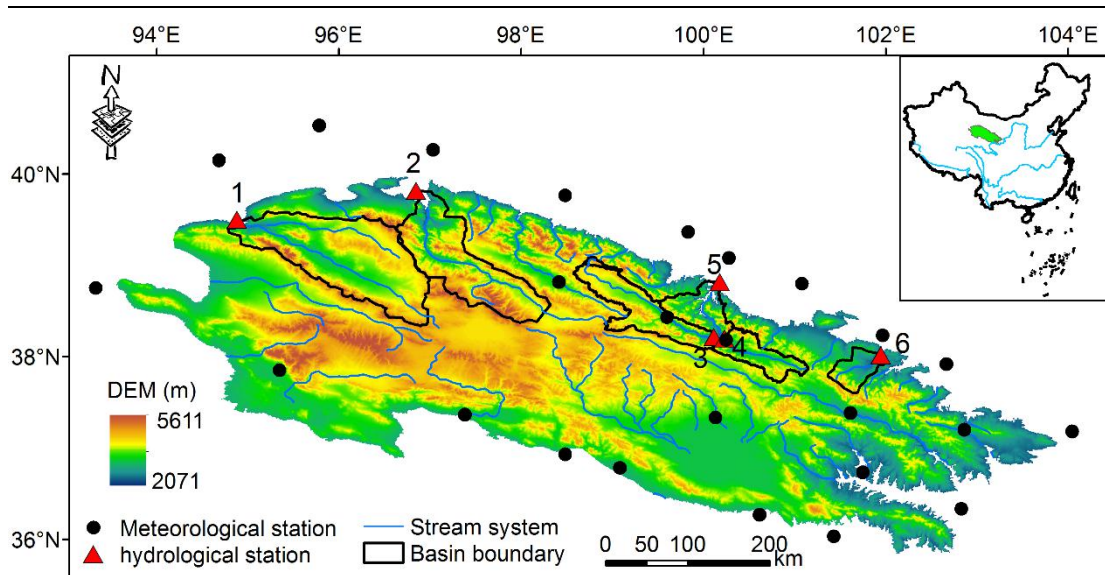
95 The overall objective of this study was to decompose the *ET* variance into the
96 temporal variability of multiple factors considering vegetation and snowmelt change.
97 The six cold alpine basins in the Qilian Mountains of northwest China were taken as
98 an example study area. Specifically, we aimed to: (i) determine the dominant driving
99 factor controlling the *ET* variance; (2) investigate the roles of vegetation and
100 snowmelt change in the variance; and (3) understand the interactions among the
101 controlling factors in *ET* variance. The proposed method will help quantify the
102 hydrological response to changes in snowmelt and vegetation in snowmelt-dependent
103 regions, and our results will prove to be insightful for water resource management in
104 other similar regions worldwide.

105 **2 Materials**

106 **2.1 Study area**

107 Six sub-basins located in the upper reaches of the Heihe, Shiyang, and Shule rivers in
108 the Qilian Mountains were chosen as the study area (Figure 1). They are important
109 inland rivers in the dry region of northwest China. The runoff generated from the
110 upper reaches contributes to nearly 70% of the water resources of the entire basin and

111 thus plays an important role in supporting agriculture, industry development, and
112 ecosystem maintenance in the middle and downstream rivers (Cong et al., 2017;
113 Wang et al., 2010a). Snowmelt and in-mountain-generated rainfall make up the water
114 supply system for the upper basins (Matin and Bourque, 2015), and the annual
115 average P exceeds 450 mm in this region. At higher altitudes, as much as 600–700
116 mm of P can be observed (Yang et al., 2017). Nearly 70% of the total rainfall
117 concentrates between June and September, while only 19% of the total rainfall occurs
118 from March to June. Snowmelt runoff is an important water source (Li et al., 2012; Li
119 et al., 2018; Li et al., 2016); in the spring, 70% of the runoff is supplied by snowmelt
120 water (Wang and Li, 2001). Characterised by a continental alpine semi-humid climate,
121 alpine desert glaciers, alpine meadows, forests, and upland meadows are the
122 predominant vegetation distribution patterns (Deng et al., 2013). Furthermore, this
123 region has experienced substantial vegetation changes and resultant hydrological
124 changes in recent decades (Bourque and Mir, 2012; Du et al., 2019; Ma et al., 2008).



125

126 Figure 1 The six basins in China's northern Qilian Mountains. The Digital elevation data, at
 127 30 m resolution, was provided by the Geospatial Data Cloud site, Computer Network Information
 128 Center, Chinese Academy of Sciences.

129 **2.2 Data**

130 Daily climate data were collected for 25 stations distributed in and around the Qilian
 131 Mountains from the China Meteorological Administration. They comprised rainfall,
 132 air temperature, sunshine hours, and relative humidity and would be used to calculate
 133 the monthly E_0 using the Priestley and Taylor (1972) equation.

134 The monthly runoff at the Dangchengwan, Changmabu, Zhamashike, Qilian,
 135 Yingluoxia, and Shagousi hydrological stations were obtained for 2001–2014 from
 136 the Bureau of Hydrology and Water Resources, Gansu Province. The sum of the
 137 monthly soil moisture and plant canopy surface water with a resolution of $0.25^\circ \times$

138 0.25° from the Global Land Data Assimilation System (GLDAS) Noah model was
139 used to estimate the total water storage. The monthly ΔS was calculated as the water
140 storage difference between two neighbouring months. Eight-day composites of the
141 MODIS MOD10A2 Version 6 snow cover product from the MODIS TERRA satellite
142 were used to produce the monthly snow cover area (*SCA*) of each basin. The *SCA* data
143 were used to drive the snowmelt runoff model.

144 A monthly normalised difference vegetation index (*NDVI*) at a spatial resolution of 1
145 km from the MODIS MOD13A3.006 product was used to assess the vegetation
146 coverage (*M*), which can be calculated from the method of Yang et al. (2009):

$$147 \quad M = \frac{NDVI - NDVI_{min}}{NDVI_{max} - NDVI_{min}} \quad (3)$$

148 ~~where $NDVI_{max}$ and $NDVI_{min}$ are the $NDVI$ values of dense forest (0.80) and bare soil~~
149 ~~(0.05). A land-use map with 1-km resolution in 2010 was used to determine the forest~~
150 ~~area of each basin, and it was provided by the Data Centre for Resources and~~
151 ~~Environmental Sciences of the Chinese Academy of Sciences. The percentages of~~
152 ~~forestland area to the whole basin area served as the F for each basin (%).~~

153 ~~ET from dataset of “ground truth of land surface evapotranspiration at regional scale~~
154 ~~in the Heihe River Basin (2012-2016) ET_{map} Version 1.0” (hereafter “ ET_{map} ”), was~~
155 ~~used to validate the reliability of our estimated ET . This dataset was published by~~
156 ~~National Tibetan Plateau Data Center. It was upscaled from 36 eddy covariance flux~~
157 ~~tower sites (65 site years) to the regional scale with five machine learning algorithms,~~
158 ~~and then applied to estimate ET for each grid cell (1 km \times 1 km) across the Heihe~~

159 River Basin each day over the period 2012–2016. It has been evaluated to have high
160 accuracy (Xu et al., 2018). Basins 3,4,5 in our study belongs to the headwater
161 sub-basins of Heihe River, and our monthly ET from April to September during
162 2012-2014 was thus compared with ET_{map} .

163 –

164 **3 Methods**

165 **3.1 The Budyko framework at monthly scales**

166 Probing the ET variability in the growing season can provide basic scientific reference
167 points for agricultural activities and water resource planning and management (Li et
168 al., 2015; Wagle and Kakani, 2014). Thus, we focus on the growing season ET
169 variability on a monthly scale in this study.

170 Among the mathematical forms of the Budyko framework, this study employed the
171 function proposed by Choudhury (1999) and Yang et al. (2008) to assess the basin
172 water balance for good performance (Zhou et al., 2015):

$$173 \quad ET = \frac{P_e \times E_0}{(P_e^n + E_0^n)^{1/n}} \quad ET = \frac{P \times E_0}{(P^n + E_0^n)^{1/n}} \quad (34)$$

174 where n is the controlling parameter of the Choudhury–Yang equation. P_e is the total
175 available water supply for ET . In previous studies, P_e included P and ΔS ($P_e = P - \Delta S$) on

176 finer time scale (Liu et al., 2019; Zeng and Cai, 2015; Zhang et al., 2016a). But
 177 snowmelt runoff should also be considered in the snow-dependent basins, and P is the
 178 total available water supply for ET. In Equation 2, however, the available water
 179 supply (P_e) includes the rainfall, snowmelt runoff, and water storage change in the
 180 snow-dependent basins on a finer time scale, which can be rewritten as Thus, P_e can
 181 be defined as:

$$P_e = R + Q_s - \Delta S. \quad (45)$$

183 Equation 3-4 can thus be redefined as follows:

$$ET_i = \frac{(R_i + Q_{s_i} - \Delta S_i) \times E_{0_i}}{((R_i + Q_{s_i} - \Delta S_i)^n + E_{0_i}^n)^{1/n}}, \quad (56)$$

185 where i indicates each month of the growing season (April to September). After
 186 estimating the monthly ET of the growing season using Equation 2, the values of n for
 187 each month can be obtained via Equation 56.

188 3.2 Estimating the equivalent of snowmelt runoff

189 With the developed relationship between snowmelt and air temperature (Hock, 2003),
 190 the degree-day model simplifies the complex processes and performs well, so it is
 191 widely used in snowmelt estimation (Griessinger et al., 2016; Rice et al., 2011;
 192 Semadeni-Davies, 1997; Wang et al., 2010a). This study estimated the monthly Q_s
 193 using the degree-day model following the Wang et al. (2015) procedure. Specifically,

194 the water equivalent of snowmelt (W , mm) during the period m can be calculated as:

$$195 \quad \sum_{i=1}^m W_i = DDF \sum_{i=1}^m T_i^+, \quad (67)$$

196 where DDF denotes the degree-day factor ($\text{mm/day} \cdot ^\circ \text{C}$), and T^+ is the sum of the
197 positive air temperatures of each month. After obtaining W , the monthly Q_s of each
198 elevation zone can be expressed as:

$$199 \quad \sum_{i=1}^m Q_{Si} = \sum_{i=1}^m W_i SCA_i, \quad (78)$$

200 where SCA_i is the snow cover area of each elevation zone.

201 According to Gao et al. (2011), the DDF values of Basins 1–6 were set to 3.4, 3.4, 4.0,
202 4.0, 4.0, and 1.7 $\text{mm/day} \cdot ^\circ \text{C}$, respectively. The six basins were divided into seven
203 elevation zones with elevation differences of 500 m. The sum of Q_s in each elevation
204 zone could be considered as the total Q_s of each basin. Previous studies have found
205 that the major snow melting period is from March to July in this area (Wang and Li,
206 2005; Wu et al., 2015); furthermore, the MODIS snow product also showed that the
207 SCA decreased significantly at the end of July. Thus, the snowmelt runoff from April
208 to July for the growing season was estimated in this study.

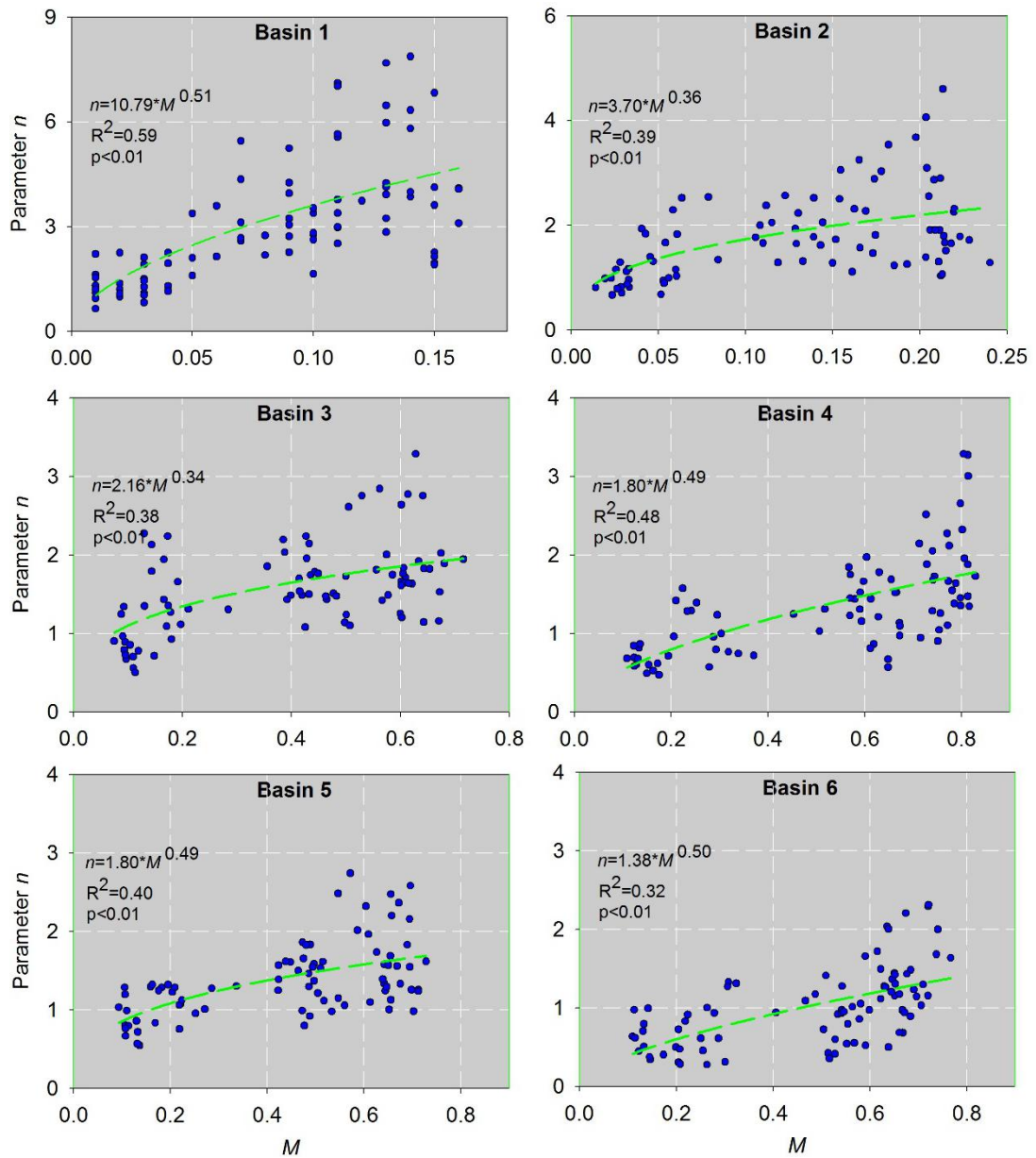
209 **3.3 Relationship between the Budyko controlling parameter and vegetation**
210 **change**

211 The relationships between the monthly parameters n and M for each basin in the
212 growing season for 2001–2014 are presented in Figure 2. It can be seen that parameter
213 n was significantly positively related to M in all six basins ($p < 0.05$), which means
214 that ET increased with increasing vegetation conditions under the given climate
215 conditions.

216 In Equation [56](#), when $n \rightarrow 0$, $ET \rightarrow 0$, which means M should have the following
217 limiting conditions: if $ET \rightarrow 0$, $T \rightarrow 0$ (transpiration), and thus $M \rightarrow 0$. Considering the
218 relationship shown in Figure 2 and the above limiting conditions, the general form of
219 parameter n can be expressed [as follows by power function followed previous studies](#)
220 [\(Liu et al., 2018; Ning et al., 2017; Yang et al., 2007\)](#):

$$221 \quad n = a \times M^b, \quad (89)$$

222 where a and b are constants, and their specific values for each basin are fitted in
223 Figure 2.



224

225 Figure 2 Relationships between the parameter n and the vegetation coverage for each basin on a

226

monthly scale.

227 3.4 ET variance decomposition

228 Liu et al. (2019) proposed a framework to identify the driving factors behind the

229 temporal variance of Q_r by combining the unbiased sample variance of Q_r with the

230 total differentiation of Q_r changes. Here, we extended this method by considering the
 231 effects of changes in snowmelt runoff and vegetation coverage on ET variance.

232 By combining Equation 5-6 with Equation 89, Equation 5-6 can be simplified as $ET \approx$
 233 $f(R_i, Q_{si}Q_{mi}, \Delta S_i, E_{0i}, M_i)$. Thus, the total differentiation of ET changes can be
 234 expressed as:

$$235 \quad dET_i = \frac{\partial f}{\partial R} dR_i + \frac{\partial f}{\partial Q_s} dQ_{smi} + \frac{\partial f}{\partial \Delta S} d\Delta S_i + \frac{\partial f}{\partial E_0} dE_{0i} + \frac{\partial f}{\partial M} dM_i + \tau, \quad (910)$$

236 where τ is the error. ~~$\frac{\partial f}{\partial R}, \frac{\partial f}{\partial Q_m}, \frac{\partial f}{\partial \Delta S}, \frac{\partial f}{\partial E_0}, \frac{\partial f}{\partial M}$ are the τ is the error.~~ The partial
 237 differential coefficients of ET to $R, Q_m, \Delta S, E_0$ and M , respectively, which can be
 238 calculated as:

$$239 \quad \frac{\partial ET}{\partial R} = \frac{\partial ET}{\partial Q_m Q_s} = -\frac{\partial ET}{\partial \Delta S} = \frac{ET}{P_e} \times \left(\frac{E_0^n}{P_e^n + E_0^n} \right), \quad (10a11a)$$

$$240 \quad \frac{\partial ET}{\partial E_0} = \frac{ET}{E_0} \times \left(\frac{P_e^n}{P_e^n + E_0^n} \right), \quad (10b11b)$$

$$241 \quad \frac{\partial ET}{\partial M} = \frac{ET}{n} \left(\frac{\ln(P_e^n + E_0^n)}{n} - \frac{P_e^n \ln P_e + E_0^n \ln E_0}{P_e^n + E_0^n} \right) \times a \times b \times M^{b-1}. \quad (10c11c)$$

242 The first-order approximation of ET changes in Equation 9-10 can be expressed as:

$$243 \quad \Delta ET_i \approx \varepsilon_1 \Delta R_i + \varepsilon_2 \Delta Q_{s_i} + \varepsilon_3 \Delta S_i + \varepsilon_4 \Delta E_{0_i} + \varepsilon_5 \Delta M_i, \quad (112)$$

$$244 \quad \text{where } \varepsilon_1 = \frac{\partial ET}{\partial R}, \varepsilon_2 = \frac{\partial ET}{\partial Q_s}, \varepsilon_3 = \frac{\partial ET}{\partial \Delta S}, \varepsilon_4 = \frac{\partial ET}{\partial E_0}, \varepsilon_5 = \frac{\partial ET}{\partial M}.$$

245 The unbiased sample variance of ET is defined as:

$$246 \quad \sigma_{ET}^2 = \frac{1}{N-1} \sum_{i=1}^N (ET_i - \overline{ET})^2 = \frac{1}{N-1} \sum_{i=1}^N (\Delta ET_i)^2. \quad (4213)$$

247 where \overline{ET} is the long term monthly mean of ET . N is the sample size, it equals 84 in
 248 this study (6 months/year×14 years=84 months). i is used to index time series of
 249 month from 1 to N .

250 Combining Equation 41-12 with Equation 4213, σ_{ET}^2 can be decomposed as the
 251 contribution from different variance/covariance sources:

$$252 \quad \sigma_{ET}^2 = \sum_{i=1}^N (\varepsilon_1 \Delta R_i + \varepsilon_2 \Delta Q_{s_i} + \varepsilon_3 \Delta S_i + \varepsilon_4 \Delta E_{0_i} + \varepsilon_5 \Delta M_i)^2. \quad (4314)$$

253 Expanding Equation 4314, σ_{ET}^2 can be further rewritten as:

$$254 \quad \sigma_{ET}^2 = \varepsilon_1^2 \sigma_R^2 + \varepsilon_2^2 \sigma_{Q_s}^2 + \varepsilon_3^2 \sigma_{\Delta S}^2 + \varepsilon_4^2 \sigma_{E_0}^2 + \varepsilon_5^2 \sigma_M^2 + 2\varepsilon_1 \varepsilon_2 \text{cov}(R, Q_s) +$$

$$255 \quad 2\varepsilon_1 \varepsilon_3 \text{cov}(R, \Delta S) + 2\varepsilon_1 \varepsilon_4 \text{cov}(R, E_0) + 2\varepsilon_1 \varepsilon_5 \text{cov}(R, M) + 2\varepsilon_2 \varepsilon_3 \text{cov}(Q_s, \Delta S) +$$

$$256 \quad 2\varepsilon_2 \varepsilon_4 \text{cov}(Q_s, E_0) + 2\varepsilon_2 \varepsilon_5 \text{cov}(Q_s, M) + 2\varepsilon_3 \varepsilon_4 \text{cov}(E_0, \Delta S) + 2\varepsilon_3 \varepsilon_5 \text{cov}(M, \Delta S) +$$

$$257 \quad 2\varepsilon_4 \varepsilon_5 \text{cov}(E_0, M), \quad (4415)$$

258 where σ represents the standard deviation, and cov represents the covariance.

259 Equation 44-15 can be further simplified as:

$$260 \quad \sigma_{ET}^2 = F(R) + F(Q_s) + F(\Delta S) + F(E_0) + F(M) + F(R_{Q_s}) + F(R_{\Delta S}) +$$

$$261 \quad F(R_{E_0}) + F(R_M) + F(Q_s_{\Delta S}) + F(Q_s_{E_0}) + F(Q_s_M) + F(\Delta S_{E_0}) +$$

$$262 \quad F(\Delta S_M) + F(E_0_M), \quad (4516)$$

Where F is the individual contributions of each factor; each two factors linked by underscore represents the interaction effects between them.

By separating out Equation 4516, the contribution of each factor to σ_{ET}^2 can be calculated as:

$$C(X_j) = \frac{F(X_j)}{\sigma_{ET}^2} \times 100\%, \quad (4617)$$

where $C(X_j)$ is the contribution of factor $F(j)$ to σ_{ET}^2 , and $j = 1-15$, representing the 15 factors in Equation 4516.

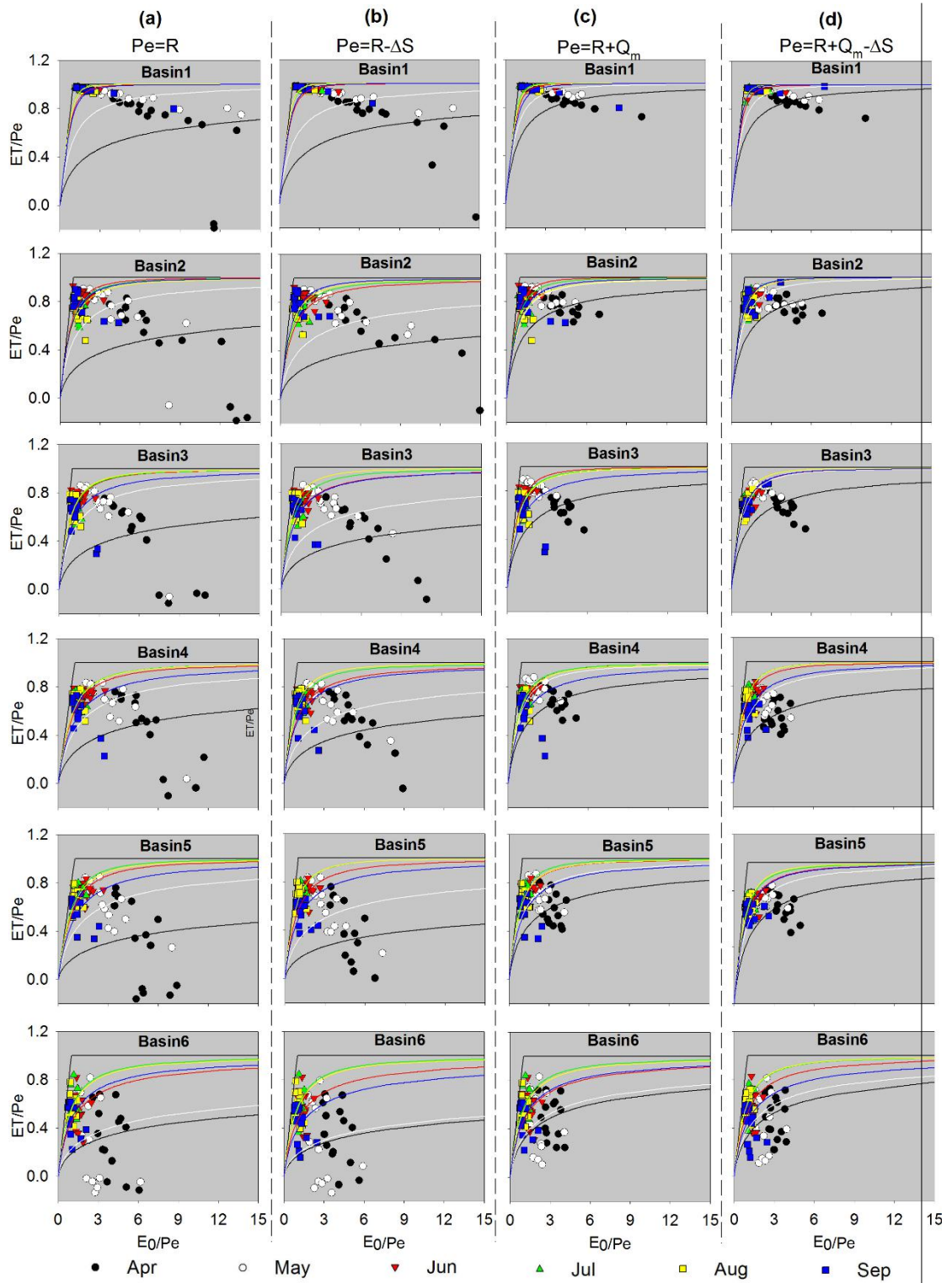
4 Results and Discussion

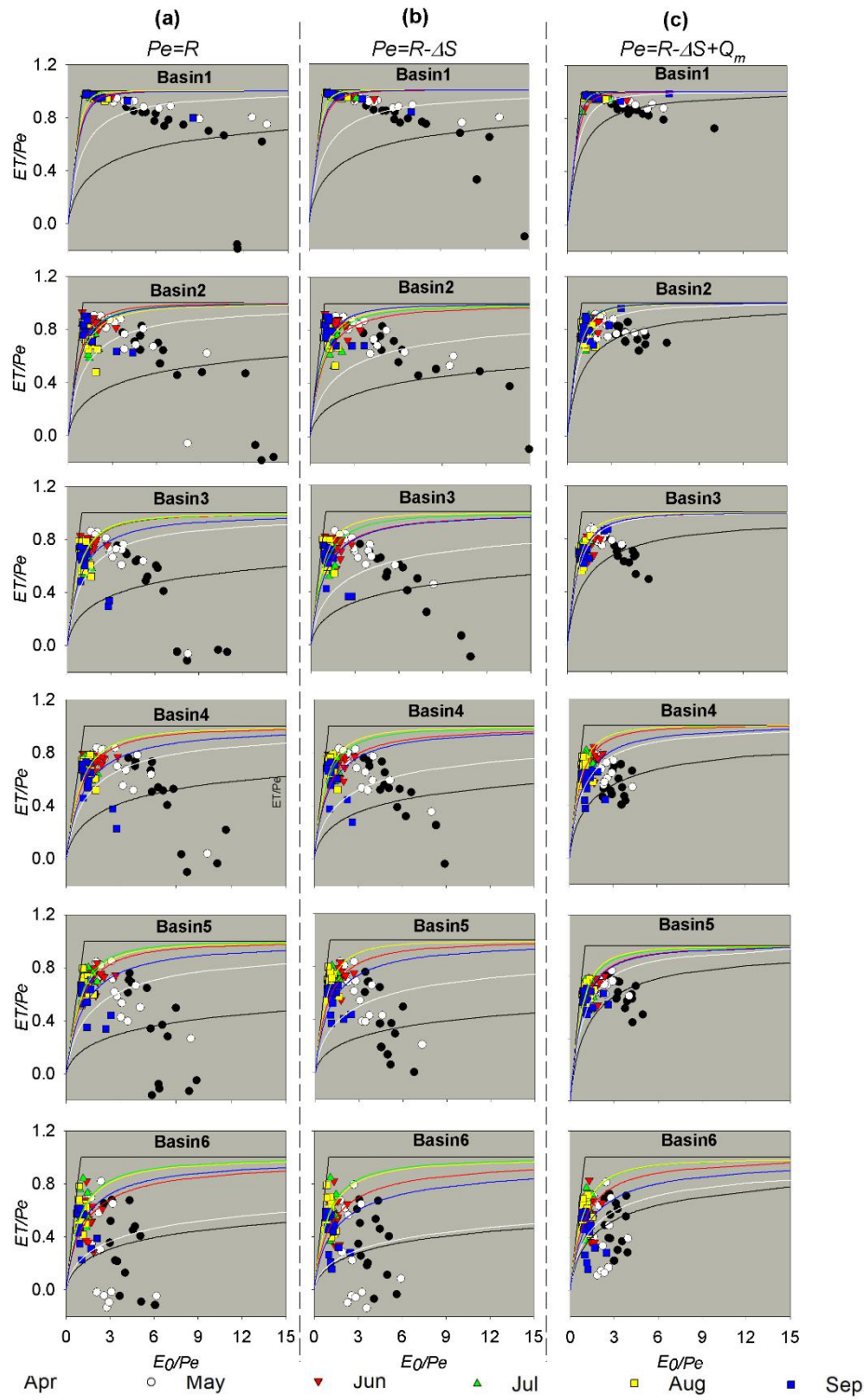
4.1 The effects of monthly storage change and snowmelt runoff in the Performance of the monthly Budyko framework

The Budyko framework is usually used for analyses of long-term average catchment water balance; however, it was employed for the interpretation of the monthly variability of the water balance in this study. Thus, it's very necessary to validate the feasibility of Budyko equation for monthly variability. Furthermore, ~~The impact of ΔS on the representation of the importance of considering ΔS in the~~ Budyko framework on a finer time-scale has been assessed ~~underscored~~ by several studies (Chen et al., 2013; Du et al., 2016; Liu et al., 2019; Zeng and Cai, 2015).; ~~H~~however, the impact effects of Q_m and its combined effects with ΔS in snowmelt-dependent basins are

281 mostly ignored. Therefore, we present the water balance in the monthly scale of six
282 basins in the Budyko's framework with three different computations of aridity index
283 ($\phi = E_0/P_e$) or ET ratio (ET/P_e) in Figure 3. In Figure 3a, $ET = R - Q_r$ when R is
284 considered as water supply, i.e., $P_e = R$. The points of monthly ET ratio and aridity
285 index in April and May were well below Budyko curves in 6 basins; monthly ET ratio
286 was even negative in several year, which means the local rain are not the only sources
287 of ET in this area, especially in spring. In Figure 3b, $ET = R - \Delta S - Q_r$ with $P_e = R - \Delta S$.
288 Compared with figure 3a, the way-off points in April and May were improved to a
289 certain extent but negative points still existed, suggesting that except for R , ΔS also
290 play a significant role in maintaining spring ET , but the variability of ET cannot be
291 completely explained by these two variables. In Figure 3c, $ET = R - \Delta S + Q_m - Q_r$ with
292 $P_e = R - \Delta S + Q_m$. Compared to the points in Figures 3a-b, all points focused on
293 Budyko's curves more closely in each basin when $P_e = R + Q_m - \Delta S$. From this
294 comparison, it can be concluded that the Budyko framework is applicable to the
295 monthly scale in snowmelt-dependent basins, if the water supply is described
296 accurately by considering ΔS and Q_m . Here, the monthly Budyko curves—scaled by
297 different available water supply values (P_e) for monthly series in the growing
298 season—were compared. When $P_e = R$ and $P_e = R - \Delta S$, the data points of the monthly
299 ET ratio and aridity index ($\phi = E_0/P_e$) in April and May were well below the Budyko
300 curves in the six sub-basins; the monthly ET ratio was even negative during several
301 years (Figure 3a,b), which means that local rain and water storage are not the only

302 sources of ET in this area, especially in the spring. When $P_e = R + Q_m$, the outlier
303 points in April and May were significantly improved (Figure 3c), suggesting that Q_m
304 is an important source of spring ET . Similarly, Wang and Li (2001) also determined
305 that 70% of the runoff is supplied by snowmelt water in the spring in this area.
306 Compared to the points in Figures 3a–c, all the points focused on Budyko's curves
307 more closely in each basin when $P_e = R + Q_m = \Delta S$ (Figure 3d). Therefore, considering
308 Q_m and ΔS in the water balance equation can improve the performance of the Budyko
309 framework in snowmelt-dependent basins on a monthly scale.





311

312

Figure 3 Plots for the aridity index vs. evapotranspiration index scaled by the available water

313

supply for monthly series in the growing season. The total water availability is (a) R , (b) $R - \Delta S$,

314

(c) $R + Q_m$, and (d) $R + Q_m - \Delta S$. The n value for each Budyko curve is fitted by long-term

315 averaged monthly data.

316 4.2 Variations in the growing season water balance

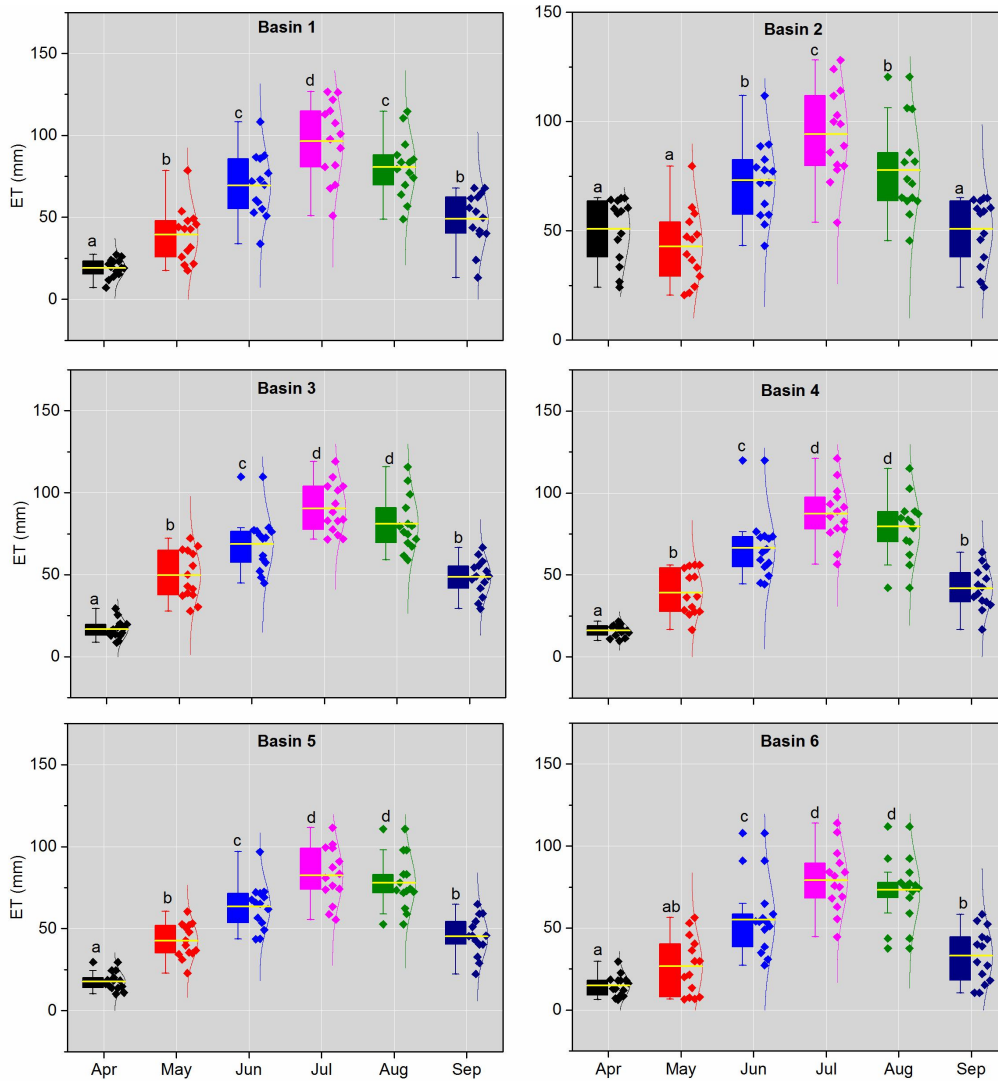
317 The mean and standard deviation (σ) for each item in the growing season water
318 balance in the six basins are summarised in Tables 1 and 2. The proportion of ΔS in
319 the water balance was small, with a mean value of 1.2 mm; however, its intra-annual
320 fluctuation was relatively large, with a $\sigma_{\Delta S}$ of 5.3 mm, and $\sigma_{\Delta S}$ was even as high as
321 9.0 mm in Basin 6. Compared to ΔS , Q_m represented a larger proportion of the water
322 balance with a mean of 8.5 ± 6.5 mm, indicating its important role in the basin water
323 supply. For this region, the water supply of ET was not only R but also included Q_m
324 and ΔS . Consequently, the mean monthly ET generally approached R (55.8 ± 27.4 mm)
325 or higher values in Basin 1.

326 Table 1 Averaged monthly hydrometeorological characteristics and vegetation coverage in the
327 growing season (2001–2014).

ID	Station	Area	R	Q_m	ΔS	E_0	M	n	E
1	Dangchengwan	14325	57.2	8.6	0.7	126.7	0.08	3.08	59.1
2	Changmabu	10961	68.9	10.8	1.1	123.0	0.13	1.79	59.3
3	Zhamashike	4986	73.5	10.6	1.5	120.3	0.40	1.59	59.1
4	Qilian	2452	74.5	9.0	1.4	116.8	0.44	1.37	54.9
5	Yingluoxia	10009	77.2	7.4	1.1	117.4	0.53	1.35	55.1
6	Shagousi	1600	83.5	4.8	1.4	116.3	0.48	1.01	47.1

328 The change patterns of the monthly R , ΔS , Q_m , and ET during the growing season are
329 presented in Figure 4 and Supplementary Figures S1–S3. R exhibited a regular

330 unimodal trend, with a maximum value occurring in July. The maximum Q_m appeared
331 in May, which is a result that is in agreement with previous studies in this region
332 (Wang and Qin, 2017; Zhang et al., 2016c). The peak of ΔS lagged that of Q_m for one
333 month in Basins 1–4 and three months in Basins 5–6, indicating a recharge of soil
334 water by snowmelt. Yang et al. (2015) also detected the time differences between ΔS
335 and Q_m and found that ΔS had a time lag of 3–4 months more than did Q_m in the Tarim
336 River Basin, another arid alpine basin in north-western China with hydroclimatic
337 conditions similar to those of the study region. Further, the abundant R in July should
338 contribute to more available water for ΔS ; however, the ΔS in July was relatively
339 small. This can be partially explained by the higher water consumption, i.e. the ET in
340 July. In a manner similar to the change pattern of R , ET exhibited a unimodal trend,
341 suggesting the crucial role of R .



342

343 Figure 4 Variations in the monthly *ET* for each basin during 2001–2014. A distribution curve is

344 shown to the right side of each box plot, and the data points are represented by diamonds.

345 Different letters indicate significant differences at $p < 0.05$.

346 4.3 Controlling factors of the *ET* variance

347 The contributions of R , E_0 , Q_m , ΔS , and M to σ_{ET}^2 for each basin are shown in Figure

348 5. The results showed that the variance of these five factors could explain σ_{ET}^2 , with

349 the total contribution rates ranging from 56.5% (Basin 6) to 98.6% (Basin 1). With the

350 decreasing ϕ from Basin 1 to Basin 6, $C(R)$ showed an increasing trend, ranging from
351 40.6% to 94.2%; conversely, $C(E_0)$ exhibited a decreasing trend, ranging from 0.2%
352 to 4.1%. This result indicated that R played a key role in σ_{ET}^2 in this region. Similarly,
353 Zhang et al. (2016a) found that $C(P)$ increased rapidly with increasing ϕ , whereas
354 $C(E_0)$ decreased rapidly based on 282 basins in China. Our results are also consistent
355 with previous conclusions that changes in ET or Q_r are dominated by changes in water
356 conditions rather than by energy conditions in dry regions (Berghuijs et al., 2017;
357 Yang et al., 2006; Zeng and Cai, 2016; Zhang et al., 2016a).

358 The M variance had the second largest contribution to σ_{ET}^2 with a mean $C(M)$ value
359 of 4.3% for the six basins. Specifically, $C(M)$ showed an increasing trend from 0.5%
360 to 9.5% with the decreasing ϕ , implying that the contribution of vegetation change to
361 ET variance was larger in relatively humid basin. It can be explained that transpiration
362 is more sensitive to vegetation change, and thus the higher vegetation coverage could
363 increase the proportion of transpiration to ET in humid regions (Niu et al., 2019;
364 Zhang et al., 2020). The Budyko hypothesis stated that change in ET is controlled by
365 change in available energy when water supply is not a limiting factor under humid
366 conditions (Budyko, 1974; Yang et al., 2006). The increasing M results in the
367 reallocation of available energy between canopy and soil. Specifically, more energy is
368 consumed by canopy thus increases transpiration. Further, Previous studies have
369 found that ET differs greatly among species, because of the difference in canopy

370 roughness, the timing of physiological functioning, water holding capacity of the soil
371 and rooting depth of the vegetation (Baldocchi et al., 2004; Bruemmer et al., 2012).
372 Generally, forest had larger ET than grassland (Ma et al., 2020; Zha et al., 2010). The
373 fraction of forest area is relatively high and thus lead to the higher contributions to ET
374 for whole basin in the humid region. For example, Wei et al. (2018) showed that the
375 global average variation in the annual Q_r due to the vegetation cover change was
376 $30.7\pm 22.5\%$ in forest-dominated regions on long-term scales, which was higher than
377 our results because of their higher forest cover.

378 ~~$C(M)$ showed an increasing trend from 0.5% to 9.5% with decreasing ϕ , implying that~~
379 ~~the contribution of the vegetation change to the ET variance was larger in the humid~~
380 ~~basin. This can be explained by the fact that better vegetation conditions, especially~~
381 ~~forest cover, could have a stronger impact on ET variance. With the estimated~~
382 ~~percentages of forestland relative to the whole basin (F) (Table S1), we found that the~~
383 ~~M variance indeed had a larger contribution to σ_{ET}^2 in Basins 4–6 with a higher F .~~
384 ~~Wei et al. (2018) showed that the global average variation in the annual Q_r due to the~~
385 ~~vegetation cover change was $30.7\pm 22.5\%$ in forest-dominated regions on long-term~~
386 ~~scales, which was higher than our results because of their higher forest cover.~~

387 The contribution of the Q_m variance ranked third with a mean value of 1.8%. Similar
388 as $C(R)$, $C(Q_m)$ showed a downward trend with the decreasing ϕ , ranging from 2.9%
389 to 0.4%. Similar to $C(R)$, $C(Q_m)$ showed a downward trend from Basin 1 to Basin 6,

390 ranging from 2.9% to 0.4%. The larger $C(Q_m)$ can be explained by the larger variance
391 in Q_m in Basins 2–4 (σ values in Table 2). However, the Q_m in Basin 1 was only 8.6
392 mm, and $C(Q_m)$ was the largest in all six sub-basins (2.9%). It can be explained that
393 the contribution of each variable to σ_{ET}^2 was not only the product of the partial
394 differential coefficients, but also relied on its variance value according to Equation 14.
395 Specifically, the partial differential coefficients of 0.1 for a variable means that a 10%
396 change in that variable may result in a change in ET by 1%, which can only reflect the
397 theoretical contribution of each variable. By multiplying the variance value, the actual
398 contribution of each variable could be obtained. This is because the contribution of
399 each variable to σ_{ET}^2 was not only the product of its variance value but also relied on
400 the elasticity coefficient of σ_{ET}^2 according to Equation 13. The ε_{Q_m} value was the
401 largest in Basin 1 and thus led to the largest $C(Q_m)$. In addition, shifts in the snowmelt
402 period can also partially explain the positive contribution of the Q_m variance. Like
403 many snow-dominated regions of the world (Barnett et al., 2005), climate warming
404 shifted the timing of snowmelt earlier in the spring in the Qilian Mountains (Li et al.,
405 2012). Earlier snowmelt due to a warmer atmosphere resulted in increased soil
406 moisture and a greater proportion of Q_m to ET (Barnhart et al., 2016; Bosson et al.,
407 2012).

408 Previous studies have considered that most precipitation changes are transferred to
409 water storage (Wang and Hejazi, 2011); thus, ΔS has distinct impacts on the

410 intra-annual ET or Q_r variance in arid regions (Ye et al., 2015; Zeng and Cai, 2016;
411 Zhang et al., 2016a). However, the study region under investigation has a small $C(\Delta S)$
412 with a mean value of 1.02%, which is likely to be caused by the vegetation conditions
413 and time-scale. First, the six basins have ~~higher vegetation coverage~~
414 ~~good-vegetation~~
~~conditions~~ compared to other arid basins; consequently, plant transpiration and
415 rainfall interception consume most of the water supply and reduce the transformation
416 of rainfall to water storage. This is consistent with previous studies that showed that
417 the fractional contribution of transpiration to ET would increase with increasing
418 woody cover (Villegas et al., 2010; Wang et al., 2010b). Second, the large
419 contribution of ΔS to the intra-annual ET or Q_r variance in arid regions is mostly
420 detected at monthly scales. The smaller ΔS in the non-growing season will increase
421 the annual value of $\sigma_{\Delta S}$. However, this study focused on the growing season with a
422 smaller $\sigma_{\Delta S}$, which consequently led to a lower $C(\Delta S)$.

423 **4.4 Interaction effects between controlling factors on the ET variance**

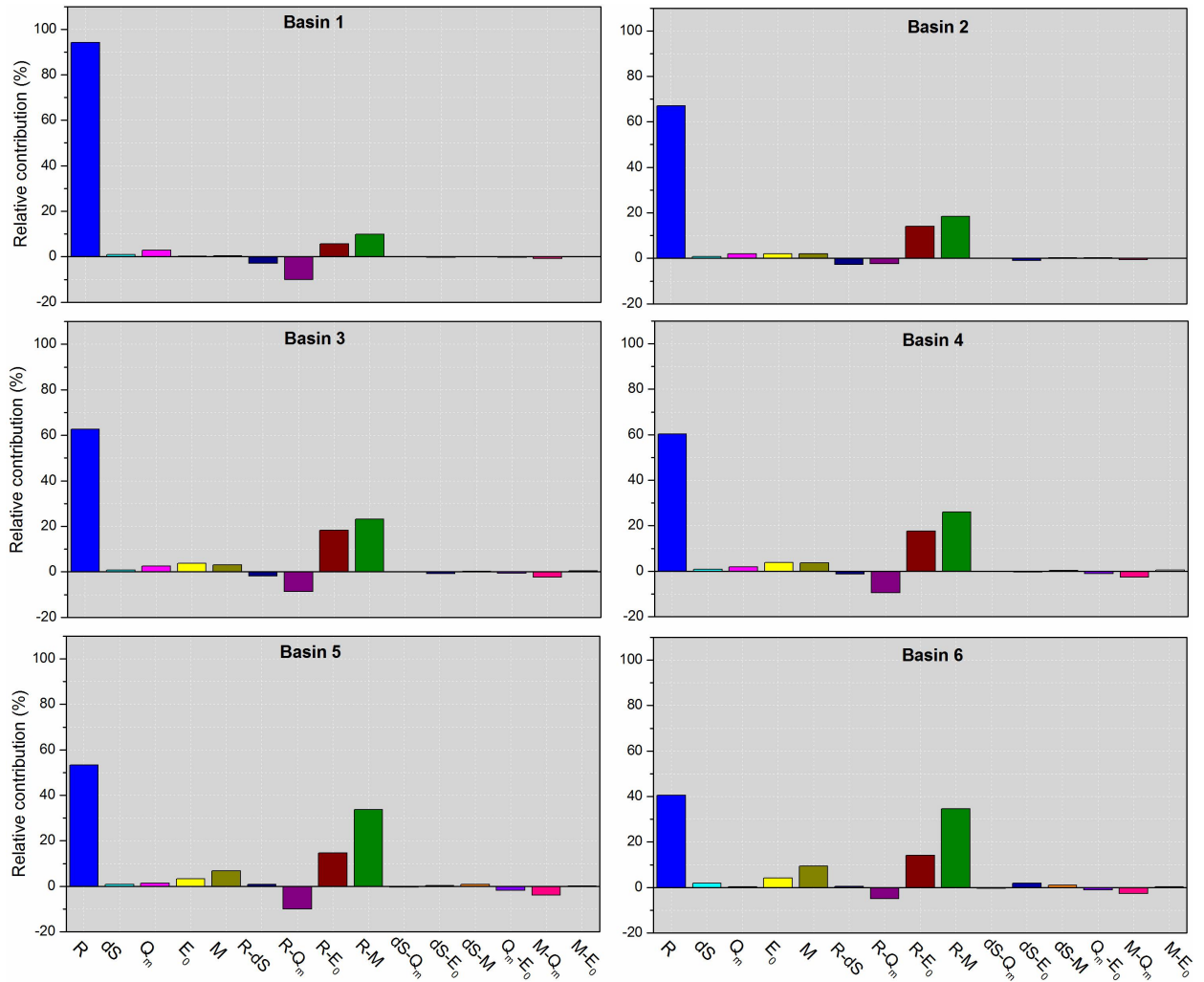
424 The interaction effect of two factors on the ET variance was represented by their
425 covariance coefficients using Equations 14 and 15 (Figure 5). Among the ten groups
426 of interaction effects, the coupled R and M had the largest contribution to the ET
427 variance, with a mean value of 24.3%. The positive covariance of R and M indicated
428 that M changes in-phase with R (i.e. R occurred in the growing season), thus
429 increasing the ET variance. $C(R_M)$ showed an increasing trend from 9.9% to 34.6%

430 with decreasing ϕ . With different water conditions, the types and proportions of the
431 main ecosystems varied across basins. In particular, F showed an increasing trend
432 with decreasing ϕ , which partially explained the spatial variations in $C(R_M)$.
433 Previous studies concluded that the differences in physiological and phenological
434 characteristics of ecosystem types are likely to modulate the response of the
435 ecosystem ET to climate variability (Bruemmer et al., 2012; Falge et al., 2002; Li et
436 al., 2019a). For example, Yuan et al. (2010) found that, at the beginning of the
437 growing season, a significantly higher ET was observed in evergreen needleleaf
438 forests; however, during the middle term of the growing season (June–August), the
439 ET was largest in deciduous broadleaf forests in a typical Alaskan basin.

440 As an indicator of climate seasonality, the covariance of R and E_0 indicates matching
441 conditions between the water and energy supplies, such as the phase difference
442 between the storm season and warm season. A positive $\text{cov}(R, E_0)$ suggests an
443 in-phase R change with E_0 and consequently increases the ET variance. In this study,
444 following $C(R_M)$, the coupled R and E_0 had a large impact on the ET variance with a
445 mean contribution of 14.1%. With a typical temperate continental climate, the study
446 area has in-phase water and energy conditions; however, its ET is limited by the water
447 supply in spite of the abundant energy supply (Yang et al., 2006). The vegetation
448 receives the largest water supply in the growing season and can vary its biomass
449 seasonally in order to adapt to the R seasonality (Potter et al., 2005; Ye et al., 2016).

450 Consequently, the impact of climate variability on ET variance was mainly reflected
451 by the R seasonality in the study area.

452 In comparison, the interacting effects between R and Q_m , M and Q_m , R and ΔS , and Q_m
453 and E_0 contributed negatively to the ET variance. Among them, the effect of the
454 coupled R and Q_m was largest with a $C(R_Q_m)$ of -7.6% . This may suggest that Q_m
455 changes were out-of-phase with R . Specifically, the major snow melting period was
456 from March to May, when snowmelt water accounts for $\sim 70\%$ of the water supply;
457 however, $\sim 65\%$ of the annual R occurred in the summer (June–August) (Li et al.,
458 2019a). Overall, Q_m sustains the ET in the spring, but R supports the ET in the
459 summer.



460

461 Figure 5 Contribution to the *ET* variance in the growing season from each component in Equation

462

15.

463 **4.5 Uncertainties**

464 Uncertainties from different sources may result in errors for this study. First, this
 465 study estimated ΔS and Q_m with the GLDAS Noah land surface model and the
 466 degree-day model, respectively. Although the GLDAS ΔS has been widely used in
 467 hydrological studies, it ignores the change in deep groundwater (Nie et al., 2016; Syed

468 et al., 2008; Zhang et al., 2016), which may lead to errors in ET estimation based on
469 water balance equation. But previous studies showed that the groundwater change in
470 our study area is relatively small, and can thus be ignored. For example, Du et al.
471 (2016) used the abcd model to quantitatively determine monthly variations of water
472 balance for the sub-basins of Heihe River (including basins 3-5 in our study) and
473 found that the soil water storage change have obvious effects on the monthly water
474 balance, whilst the impact of monthly groundwater storage change is negligible.
475 Furthermore, it has been found that any change in climate conditions and underlying
476 basin characteristics will affect the contributions of heat balance components and
477 cause temporal variations of DDF (Kuusisto, 1980; Ohmura, 2001). But previous
478 studies indicated that there is no significant seasonal change in DDF in west China
479 (Zhang et al., 2006); as such, it is acceptable to estimate snowmelt runoff using fixed
480 DDF values in this study. In comparison, the contribution of snow meltwater to runoff
481 (F_s) was 12.9% in Basin 2 during 1971-2015 by using Spatial Processes in Hydrology
482 model(Li et al., 2019), while F_s was 25% in Basin 3 from 2001 to 2012 based on
483 geomorphology-based ecohydrological model (Li et al., 2018), <10% in Basin 6
484 during 1961-2006 by using SRM model (Gao et al., 2011). Our results indicated that
485 the F_s in Basin 2, 3 and 6 were 14.8%, 24.5% and 6.7%, respectively, which were
486 close to those from different models. Finally, the uncertainties of ΔS and Q_m may lead
487 to errors in ET estimation by water balance equation. To validate the reliability of our
488 estimated ET , the comparison with ET_{map} from April to September during 2012-2014

489 was conducted (Figure S4). The results showed that our estimated ET fitted well with
490 ET_{map} and basically fell around the 1:1 line, indicating ET estimated using water
491 balance equation by considering the items of ΔS and Q_m is acceptable.

492 Second, previous studies concluded that three main factors could be responsible for
493 the variability of n , including underlying physical conditions (such as soil and
494 topography characteristics) (Milly, 1994; Yang et al., 2009), climate seasonality (such
495 as the temporal variability of rainfall, mismatch between water and energy) (Ning et
496 al., 2017; Potter et al., 2005) and vegetation dynamics (Donohue et al., 2007; Zhang et
497 al., 2001). On the short time scale, the changes in soil and topography are negligible
498 and its impact on the variability of n can be ignored. In consequence, the factors,
499 should be considered, are climate seasonality and vegetation dynamics. When
500 parameterizing n , this study considered M but ignored climate seasonality since the
501 covariance item between R and E_0 , i.e. $\varepsilon_1\varepsilon_4\text{COV}(R, E_0)$ in the Equation (15) can
502 represent climate seasonality. In addition, human influence represented by parameter
503 n on the water balance cannot be ignored, which remains further investigation.

504 **5 Conclusion**

505 Recently, several studies have applied a variance decomposition framework based on
506 the Budyko equation to elucidate the dominant driving factors of the ET variance at
507 annual and intra-annual scales by decomposing the intra-annual ET variance into the

508 variance/covariance of P , E_0 , and ΔS . Vegetation changes can greatly affect the ET
509 variability, but their effects on the ET variance on finer time-scales was not quantified
510 by this decomposed method. Further, in snow-dependent regions, snowpack stores
511 precipitation in winter and releases water in spring; thus, Q_m plays an important role
512 in the hydrological cycle. Therefore, it is also necessary to consider the role of the Q_m
513 changes on the ET variability.

514 In this study, six arid alpine basins in the Qilian Mountains of northwest China were
515 chosen as examples. The monthly Q_m during 2001–2014 was estimated using the
516 degree-day model, and the growing season ET was calculated using the water balance
517 equation ($ET = R + Q_s - Q_r - \Delta S$). The controlling parameter n of the
518 Choudhury–Yang equation was found to be closely ~~correlated~~ corrected with M , as
519 estimated by $NDVI$ data. Thus, by combining the Choudhury–Yang equation with the
520 semi-empirical formula between n and M , the growing season σ_{ET}^2 is decomposed
521 into the temporal variance and covariance of R , E_0 , ΔS , Q_m , and M . The main results
522 showed that considering Q_m and ΔS in the water balance equation can improve the
523 performance of the Budyko framework in snow-dependent basins on a monthly scale;
524 σ_{ET}^2 was primarily enhanced by the R variance, followed by the coupled R and M and
525 then the coupled R and E_0 . The enhancing effects of the variance in M and Q_m cannot
526 be ignored; however, the interactions between R and Q_m , M and Q_m , R and ΔS , and Q_m
527 and E_0 dampened σ_{ET}^2 . As a simple and effective method, our extended ET variance

528 decomposition method has the potential to be widely used to assess the hydrological
 529 responses to changes in the climate and vegetation in snow-dependent regions at finer
 530 time-scales.

531 Table 2 The elasticity coefficients of ET for five variables and the standard deviation of each
 532 variable for the six basins.

Basin	Elasticity coefficients					Standard deviation						
	ε_R	ε_{Q_m}	$\varepsilon_{\Delta S}$	ε_{E_0}	ε_M	σ_R ,	σ_{Q_m} ,	$\sigma_{\Delta S}$,	σ_{E_0} ,	σ_M	Predicted	Assessed
						mm	mm	mm	mm		σ_{ET} , mm	σ_{ET} , mm
1	0.85	0.85	-0.85	0.06	41.94	34.4	6.0	3.4	25.5	0.05	30.2	31.2
2	0.56	0.56	-0.56	0.16	55.84	40.6	7.0	4.3	24.7	0.07	27.8	30.3
3	0.46	0.46	-0.46	0.20	20.81	42.5	8.5	4.9	23.6	0.21	24.9	27.9
4	0.44	0.44	-0.44	0.19	20.58	40.1	7.2	4.8	23.1	0.21	22.5	25.8
5	0.43	0.43	-0.43	0.19	24.60	39.8	6.3	5.1	22.0	0.25	23.3	25.0
6	0.33	0.33	-0.33	0.18	31.51	41.2	4.0	9.0	23.6	0.21	21.3	24.3

533

534

535 **Data availability**

536 The Digital elevation data are available at

537 <http://www.gscloud.cn/sources/accessdata/310?pid=302>. Meteorological data are

538 available at

539 http://data.cma.cn/data/detail/dataCode/SURF_CLI_CHN_MUL_DAY_CES_V3.0.htm

540 ml. The runoff records were obtained from the Bureau of Hydrology and Water

541 Resources, Gansu Province. The GLDAS data are available at

542 https://disc.gsfc.nasa.gov/datasets/GLDAS_NOAH025_M_2.0/summary. MODIS

543 MOD10A2 Version 6 snow cover products are available at

544 <https://nsidc.org/data/mod10a2>. MODIS MOD13A3.006 products are available at

545 <https://lpdaac.usgs.gov/products/mod13a3v006/>. The dataset of “ground truth of land

546 surface evapotranspiration at regional scale in the Heihe River Basin (2012-2016)

547 ETmap Version 1.0” are available at

548 <http://data.tpdc.ac.cn/zh-hans/data/8efbb18d-bc02-4bf6-9f21-345480d6637f/?q=ETM>

549 ap.

550

551 **Author contributions**

552 Tingting Ning: Methodology, Writing–original draft, Software, Visualisation

553 Zhi Li: Writing–review & editing

554 Qi Feng: Conceptualisation, Supervision

555 Zongxing Li and Yanyan Qin: Data curation, Resources

556 **Competing interests**

557 The authors declare that they have no conflicts of interest.

558 **Acknowledgements**

559 This study was supported by the National Natural Science Foundation of China
560 (41807160), Opening Research Foundation of Key Laboratory of Land Surface
561 Process and Climate Change in Cold and Arid Regions, Chinese Academy of Sciences
562 (LPCC 2020003), the “Western Light”-Key Laboratory Cooperative Research
563 Cross-Team Project of Chinese Academy of Sciences, the CAS ‘Light of West China’
564 Program (Y929651001) the Major Program of the Natural Science Foundation of
565 Gansu Province, China (18JR4RA002) , and the Second Tibetan Plateau Scientific
566 Expedition and Research Program (STEP, Grant No.2019QZKK0405).

567 **References**

568 [Baldocchi, D.D., Xu, L.K.,&Kiang, N., 2004. How plant functional-type, weather,](#)
569 [seasonal drought, and soil physical properties alter water and energy fluxes of](#)
570 [an oak-grass savanna and an annual grassland. *Agricultural and Forest*](#)
571 [*Meteorology*, 123\(1-2\): 13-39.](#)

572 Barnett, T.P., Adam, J.C.,&Lettenmaier, D.P., 2005. Potential impacts of a warming
573 climate on water availability in snow-dominated regions. *Nature*, 438(7066):
574 303-309.

575 Barnhart, T.B., Molotch, N.P., Livneh, B., Harpold, A.A., Knowles, J.F.,&Schneider,
576 D., 2016. Snowmelt rate dictates streamflow. *Geophysical Research Letters*,
577 43(15): 8006-8016.

578 Berghuijs, W.R., Larsen, J.R., Van Emmerik, T.H.M.,&Woods, R.A., 2017. A Global
579 Assessment of Runoff Sensitivity to Changes in Precipitation, Potential
580 Evaporation, and Other Factors. *Water Resources Research*, 53: 8475-8486.

581 Bosson, E., Sabel, U., Gustafsson, L.-G., Sassner, M.,&Destouni, G., 2012. Influences
582 of shifts in climate, landscape, and permafrost on terrestrial hydrology.
583 *Journal of Geophysical Research-Atmospheres*, 117: D05120.

584 Bourque, C.P.A.,&Mir, M.A., 2012. Seasonal snow cover in the Qilian Mountains of

585 Northwest China: Its dependence on oasis seasonal evolution and lowland
586 production of water vapour. *Journal of Hydrology*, 454: 141-151.

587 Bruemmer, C., Black, T.A., Jassal, R.S., Grant, N.J., Spittlehouse, D.L., Chen, B.,
588 Nesic, Z., Amiro, B.D., Arain, M.A., Barr, A.G., Bourque, C.P.A., Coursolle,
589 C., Dunn, A.L., Flanagan, L.B., Humphreys, E.R., Lafleur, P.M., Margolis,
590 H.A., McCaughey, J.H., & Wofsy, S.C., 2012. How climate and vegetation type
591 influence evapotranspiration and water use efficiency in Canadian forest,
592 peatland and grassland ecosystems. *Agricultural and Forest Meteorology*, 153:
593 14-30.

594 Budyko, M.I., 1961. Determination of evaporation from the land surface (in Russian).
595 *Izvestiya Akad.nauk Sssr.ser.geograf.geofiz*, 6: 3-17.

596 Budyko, M.I., 1974. Climate and life. Academic, New York.

597 Chen, X., Alimohammadi, N., & Wang, D., 2013. Modeling interannual variability of
598 seasonal evaporation and storage change based on the extended Budyko
599 framework. *Water Resources Research*, 49(9): 6067-6078.

600 Choudhury, B.J., 1999. Evaluation of an empirical equation for annual evaporation
601 using field observations and results from a biophysical model. *Journal of*
602 *Hydrology*, 216(1-2): 99-110.

-
- 603 Cong, Z., Shahid, M., Zhang, D., Lei, H.,&Yang, D., 2017. Attribution of runoff
604 change in the alpine basin: a case study of the Heihe Upstream Basin, China.
605 *Hydrological Sciences Journal-Journal Des Sciences Hydrologiques*, 62(6):
606 1013-1028.
- 607 Deng, S., Yang, T., Zeng, B., Zhu, X.,&Xu, H., 2013. Vegetation cover variation in the
608 Qilian Mountains and its response to climate change in 2000-2011. *Journal of*
609 *Mountain Science*, 10(6): 1050-1062.
- 610 Donohue, R.J., Roderick, M.L. and McVicar, T.R., 2007. On the importance of
611 including vegetation dynamics in Budyko's hydrological model. *Hydrology*
612 *and Earth System Sciences*, 11(2): 983-995.
- 613 Du, C., Sun, F., Yu, J., Liu, X.,&Chen, Y., 2016. New interpretation of the role of
614 water balance in an extended Budyko hypothesis in arid regions. *Hydrology*
615 *and Earth System Sciences*, 20(1): 393-409.
- 616 Du, J., He, Z., Piatek, K.B., Chen, L., Lin, P.,&Zhu, X., 2019. Interacting effects of
617 temperature and precipitation on climatic sensitivity of spring vegetation
618 green-up in arid mountains of China. *Agricultural and Forest Meteorology*,
619 269: 71-77.
- 620 Falge, E., Baldocchi, D., Tenhunen, J., Aubinet, M., Bakwin, P., Berbigier, P.,
621 Bernhofer, C., Burba, G., Clement, R., Davis, K.J., Elbers, J.A., Goldstein,

622 A.H., Grelle, A., Granier, A., Guomundsson, J., Hollinger, D., Kowalski, A.S.,
623 Katul, G., Law, B.E., Malhi, Y., Meyers, T., Monson, R.K., Munger, J.W.,
624 Oechel, W., Paw, K.T., Pilegaard, K., Rannik, U., Rebmann, C., Suyker, A.,
625 Valentini, R., Wilson, K., & Wofsy, S., 2002. Seasonality of ecosystem
626 respiration and gross primary production as derived from FLUXNET
627 measurements. *Agricultural and Forest Meteorology*, 113(1-4): 53-74.

628 Feng, S., Liu, J., Zhang, Q., Zhang, Y., Singh, V.P., Gu, X., & Sun, P., 2020. A global
629 quantitation of factors affecting evapotranspiration variability. *Journal of*
630 *Hydrology*, 584: 124688 .

631 Feng, X., Fu, B., Piao, S., Wang, S., & Ciais, P., 2016. Revegetation in China's Loess
632 Plateau is approaching sustainable water resource limits. *Nature Climate*
633 *Change*, 6: 1019-1022.

634 Gao, X., Zhang, S., Ye, B., & Gao, H., 2011. Recent changes of glacier runoff in the
635 Hexi Inland river basin. *Advances in Water Science (In Chinese)*, 22(3):
636 344-350.

637 Godsey, S.E., Kirchner, J.W., & Tague, C.L., 2014. Effects of changes in winter
638 snowpacks on summer low flows: case studies in the Sierra Nevada, California,
639 USA. *Hydrological Processes*, 28(19): 5048-5064.

640 Griessinger, N., Seibert, J., Magnusson, J., & Jonas, T., 2016. Assessing the benefit of

641 snow data assimilation for runoff modeling in Alpine catchments. *Hydrology*
642 *and Earth System Sciences*, 20(9): 3895-3905.

643 Hock, R., 2003. Temperature index melt modelling in mountain areas. *Journal of*
644 *Hydrology*, 282(1-4): 104-115.

645 Huning, L.S.,&AghaKouchak, A., 2018. Mountain snowpack response to different
646 levels of warming. *Proceedings of the National Academy of Sciences of the*
647 *United States of America*, 115(43): 10932-10937.

648 Katul, G.G., Oren, R., Manzoni, S., Higgins, C.,&Parlange, M.B., 2012.
649 Evapotranspiration: a process driving mass transport and energy exchange in
650 the soil-plant-atmosphere-climate system. *Reviews of Geophysics*, 50:
651 RG3002.

652 Koster, R.D.,&Suarez, M.J., 1999. A simple framework for examining the interannual
653 variability of land surface moisture fluxes. *Journal of Climate*, 12(7):
654 1911-1917.

655 Kuusisto, E., 1980. On the values and variability of degree-day melting factor in
656 Finland. *Nordic Hydrology*, 11(5): 235-242.

657 Lan, Y., Hu, X., Din, H., La, C.,&Song, J., 2012. Variation of Water Cycle Factors in
658 the Western Qilian Mountain Area under Climate Warming Taking the

659 Mountain Watershed of the Main Stream of Shule River Basin for Example.
660 *Journal of Mountain Science (in Chinese)* , 30(6): 675-680.

661 Li, B., Chen, Y., Chen, Z.,&Li, W., 2012. The Effect of Climate Change during
662 Snowmelt Period on Streamflow in the Mountainous Areas of Northwest
663 China. *Acta Geographica Sinica (In Chinese)* , 67(11): 1461-1470.

664 Li, D., Pan, M., Cong, Z., Zhang, L.,&Wood, E., 2013. Vegetation control on water
665 and energy balance within the Budyko framework. *Water Resources Research*,
666 49(2): 969-976.

667 Li, H., Zhao, Q., Wu, J., Ding, Y., Qin, J., Wei, H.,&Zeng, D., 2019. Quantitative
668 simulation of the runoff components and its variation characteristics in the
669 upstream of the Shule River. *Journal of Glaciology and Geocryology (in*
670 *Chinese)*, 41(4): 907-917.

671 Li, L.L., Li, J., Chen, H.M.,&Yu, R.C., 2019a. Diurnal Variations of Summer
672 Precipitation over the Qilian Mountains in Northwest China. *Journal of*
673 *Meteorological Research*, 33(1): 18-30.

674 Li, S., Zhang, L., Kang, S., Tong, L., Du, T., Hao, X.,&Zhao, P., 2015. Comparison of
675 several surface resistance models for estimating crop evapotranspiration over
676 the entire growing season in arid regions. *Agricultural and Forest*
677 *Meteorology*, 208: 1-15.

678 Li, X., Cheng, G., Ge, Y., Li, H., Han, F., Hu, X., Tian, W., Tian, Y., Pan, X., Nian, Y.,
679 Zhang, Y., Ran, Y., Zheng, Y., Gao, B., Yang, D., Zheng, C., Wang, X., Liu,
680 S.,&Cai, X., 2018. Hydrological Cycle in the Heihe River Basin and Its
681 Implication for Water Resource Management in Endorheic Basins. *Journal of*
682 *Geophysical Research-Atmospheres*, 123(2): 890-914.

683 Li, Z., Feng, Q., Li, Z., Yuan, R., Gui, J.,&Lv, Y., 2019b. Climate background, fact
684 and hydrological effect of multiphase water transformation in cold regions of
685 the Western China: A review. *Earth-Science Reviews*, 190: 33-57.

686 Li, Z., Feng, Q., Wang, Q.J., Yong, S., Cheng, A.,&Li, J., 2016. Contribution from
687 frozen soil meltwater to runoff in an in-land river basin under water scarcity
688 by isotopic tracing in northwestern China. *Global and Planetary Change*, 136:
689 41-51.

690 Liu, J., Zhang, Q., Feng, S., Gu, X., Singh, V.P.,&Sun, P., 2019. Global Attribution of
691 Runoff Variance Across Multiple Timescales. *Journal of Geophysical*
692 *Research-Atmospheres*, 124(24): 13962-13974.

693 Liu, J., Zhang, Q., Singh, V.P., Song, C., Zhang, Y.,&Sun, P., 2018. Hydrological
694 effects of climate variability and vegetation dynamics on annual fluvial water
695 balance at global large river basins. *Hydrology & Earth System Sciences*, 22:
696 4047-4060.

697 [Ma, S., Eichelmann, E., Wolf, S., Rey-Sanchez, C.,&Baldocchi, D.D., 2020.](#)
698 [Transpiration and evaporation in a Californian oak-grass savanna: Field](#)
699 [measurements and partitioning model results. *Agricultural and Forest*](#)
700 [*Meteorology*, 295: 108204.](#)

701 Ma, Z., Kang, S., Zhang, L., Tong, L.,&Su, X., 2008. Analysis of impacts of climate
702 variability and human activity on streamflow for a river basin in arid region of
703 northwest China. *Journal of Hydrology*, 352(3-4): 239-249.

704 Matin, M.A.,&Bourque, C.P.A., 2015. Mountain-river runoff components and their
705 role in the seasonal development of desert-oases in northwest China. *Journal*
706 *of Arid Environments*, 122: 1-15.

707 Maurya, A.S., Rai, S.P., Joshi, N., Dutt, K.S.,&Rai, N., 2018. Snowmelt runoff and
708 groundwater discharge in Himalayan rivers: a case study of the Satluj River,
709 NW India. *Environmental Earth Sciences*, 77(19): 694.

710 Milly, P.C.D, 1994. Climate,soil-water storage, and the average annual water-balance.
711 *Water Resources Research*, 30(7): 2143-2156.

712 Nie, N., Zhang, W.C., Zhang, Z.J., Guo, H.D.,&Ishwaran, N., 2016. Reconstructed
713 Terrestrial Water Storage Change (Delta TWS) from 1948 to 2012 over the
714 Amazon Basin with the Latest GRACE and GLDAS Products. *Water*
715 *Resources Management*, 30(1): 279-294.

716 Ning, T., Li, Z. and Liu, W. , 2017. Vegetation dynamics and climate seasonality
717 jointly control the interannual catchment water balance in the Loess Plateau
718 under the Budyko framework. *Hydrology and Earth System Sciences*, 21(3):
719 1515-1526.

720 Ning, T., Li, Z., Feng, Q., Chen, W.,&Li, Z., 2020. Effects of forest cover change on
721 catchment evapotranspiration variation in China. *Hydrological Processes*,
722 34(10): 2219-2228.

723 Niu, Z., He, H., Zhu, G., Ren, X., Zhang, L., Zhang, K., Yu, G., Ge, R., Li, P., Zeng,
724 N.,&Zhu, X., 2019. An increasing trend in the ratio of transpiration to total
725 terrestrial evapotranspiration in China from 1982 to 2015 caused by greening
726 and warming. *Agricultural and Forest Meteorology*, 279:[107701](#).

727 Ohmura, A., 2001. Physical basis for the temperature-based melt-index method.
728 *Journal of Applied Meteorology*, 40(4): 753-761.

729 Potter, N.J., Zhang, L., Milly, P.C.D., McMahon, T.A.,&Jakeman, A.J., 2005. Effects
730 of rainfall seasonality and soil moisture capacity on mean annual water
731 balance for Australian catchments. *Water Resources Research*, 41(6): W06007.

732 Priestley, C.,&Taylor, R., 1972. On the assessment of surface heat flux and
733 evaporation using large-scale parameters. *Monthly Weather Review*, 100(2):
734 81-92.

735 Qin, Y., Abatzoglou, J.T., Siebert, S., Huning, L.S., AghaKouchak, A., Mankin, J.S.,
736 Hong, C., Tong, D., Davis, S.J., & Mueller, N.D., 2020. Agricultural risks from
737 changing snowmelt. *Nature Climate Change*, 10(5): 459-465.

738 Ragetti, S., Pellicciotti, F., Immerzeel, W.W., Miles, E.S., Petersen, L., Heynen, M.,
739 Shea, J.M., Stumm, D., Joshi, S., & Shrestha, A., 2015. Unraveling the
740 hydrology of a Himalayan catchment through integration of high resolution in
741 situ data and remote sensing with an advanced simulation model. *Advances in*
742 *Water Resources*, 78: 94-111.

743 Rice, R., Bales, R.C., Painter, T.H., & Dozier, J., 2011. Snow water equivalent along
744 elevation gradients in the Merced and Tuolumne River basins of the Sierra
745 Nevada. *Water Resources Research*, 47: W08515.

746 Rodriguez-Iturbe, I., 2000. Ecohydrology: A hydrologic perspective of
747 climate-soil-vegetation dynamics. *Water Resources Research*, 36(1): 3-9.

748 Semadeni-Davies, A., 1997. Monthly snowmelt modelling for large-scale climate
749 change studies using the degree day approach. *Ecological Modelling*, 101(2-3):
750 303-323.

751 Stewart, I.T., 2009. Changes in snowpack and snowmelt runoff for key mountain
752 regions. *Hydrological Processes*, 23(1): 78-94.

753 Stewart, I.T., Cayan, D.R., & Dettinger, M.D., 2005. Changes toward earlier
754 streamflow timing across western North America. *Journal of Climate*, 18(8):
755 1136-1155.

756 Syed, T.H., Famiglietti, J.S., Rodell, M., Chen, J., & Wilson, C.R., 2008. Analysis of
757 terrestrial water storage changes from GRACE and GLDAS. *Water Resources*
758 *Research*, 44(2): [W02433](#).

759 Villegas, J.C., Breshears, D.D., Zou, C.B., & Law, D.J., 2010. Ecohydrological controls
760 of soil evaporation in deciduous drylands: How the hierarchical effects of litter,
761 patch and vegetation mosaic cover interact with phenology and season.
762 *Journal of Arid Environments*, 74(5): 595-602.

763 Wagle, P., & Kakani, V.G., 2014. Growing season variability in evapotranspiration,
764 ecosystem water use efficiency, and energy partitioning in switchgrass.
765 *Ecohydrology*, 7(1): 64-72.

766 Wang, D., & Hejazi, M., 2011. Quantifying the relative contribution of the climate and
767 direct human impacts on mean annual streamflow in the contiguous United
768 States. *Water Resources Research*, 47: W00J12.

769 Wang, J., Li, H., & Hao, X., 2010a. Responses of snowmelt runoff to climatic change
770 in an inland river basin, Northwestern China, over the past 50 years.
771 *Hydrology and Earth System Sciences*, 14(10): 1979-1987.

-
- 772 Wang, J.,&Li, S., 2005. The influence of climate change on snowmelt runoff variation
773 in arid alpine regions of China. *Science in China (In Chinese)*, 35(7): 664-670.
- 774 Wang, J.,&Li, W., 2001. Establishing snowmelt runoff simulating model using remote
775 sensing data and GIS in the west of China. *International Journal of Remote*
776 *Sensing*, 22(17): 3267-3274.
- 777 Wang, K., Wang, P., Li, Z., Cribb, M.,&Sparrow, M., 2007. A simple method to
778 estimate actual evapotranspiration from a combination of net radiation,
779 vegetation index, and temperature. *Journal of Geophysical*
780 *Research-Atmospheres*, 112(D15): D15107.
- 781 Wang, L., Caylor, K.K., Villegas, J.C., Barron-Gafford, G.A., Breshears,
782 D.D.,&Huxman, T.E., 2010b. Partitioning evapotranspiration across gradients
783 of woody plant cover: Assessment of a stable isotope technique. *Geophysical*
784 *Research Letters*, 37: L09401.
- 785 Wang, R., Yao, Z., Liu, Z., Wu, S., Jiang, L.,&Wang, L., 2015. Snow cover variability
786 and snowmelt in a high-altitude ungauged catchment. *Hydrological Processes*,
787 29(17): 3665-3676.
- 788 Wang, Y.-J.,&Qin, D.-H., 2017. Influence of climate change and human activity on
789 water resources in arid region of Northwest China: An overview. *Advances in*
790 *Climate Change Research*, 8(4): 268-278.

-
- 791 Wei, X., Li, Q., Zhang, M., Giles-Hansen, K., Liu, W., Fan, H., Wang, Y., Zhou, G.,
792 Piao, S.,&Liu, S., 2018. Vegetation cover-another dominant factor in
793 determining global water resources in forested regions. *Global Change*
794 *Biology*, 24(2): 786-795.
- 795 Wu, C., Hu, B.X., Huang, G.,&Zhang, H., 2017. Effects of climate and terrestrial
796 storage on temporal variability of actual evapotranspiration. *Journal of*
797 *Hydrology*, 549: 388-403.
- 798 Wu, F., Zhan, J., Wang, Z.,&Zhang, Q., 2015. Streamflow variation due to glacier
799 melting and climate change in upstream Heihe River Basin, Northwest China.
800 *Physics and Chemistry of the Earth*, 79-82: 11-19.
- 801 Xu, C.Y.,&Singh, V.P., 2005. Evaluation of three complementary relationship
802 evapotranspiration models by water balance approach to estimate actual
803 regional evapotranspiration in different climatic regions. *Journal of Hydrology*,
804 308(1-4): 105-121.
- 805 Xu, T., Guo, Z., Liu, S., He, X., Meng, Y., Xu, Z., Xia, Y., Xiao, J., Zhang, Y.,&Ma, Y.,
806 2018. Evaluating Different Machine Learning Methods for Upscaling
807 Evapotranspiration from Flux Towers to the Regional Scale. *Journal of*
808 *Geophysical Research: Atmospheres*, 123: 8674-8690.
- 809 Xu, X., Liu, W., Scanlon, B.R., Zhang, L.,&Pan, M., 2013. Local and global factors

810 controlling water-energy balances within the Budyko framework. *Geophysical*
811 *Research Letters*, 40(23): 6123-6129.

812 Yang, D., Shao, W., Yeh, P.J.F., Yang, H., Kanae, S.,&Oki, T., 2009. Impact of
813 vegetation coverage on regional water balance in the nonhumid regions of
814 China. *Water Resources Research*, 45: W00A14.

815 Yang, D.W., Sun, F.B., Liu, Z.T., Cong, Z.T.,&Lei, Z.D., 2006. Interpreting the
816 complementary relationship in non-humid environments based on the Budyko
817 and Penman hypotheses. *Geophysical Research Letters*, 33(18): L18402.

818 Yang, H.B., Yang, D.W., Lei, Z.D.,&Sun, F.B., 2008. New analytical derivation of the
819 mean annual water-energy balance equation. *Water Resources Research*, 44(3):
820 W03410.

821 Yang, L., Feng, Q., Yin, Z., Wen, X., Si, J., Li, C.,&Deo, R.C., 2017. Identifying
822 separate impacts of climate and land use/cover change on hydrological
823 processes in upper stream of Heihe River, Northwest China. *Hydrological*
824 *Processes*, 31(5): 1100-1112.

825 Yang, T., Wang, C., Chen, Y., Chen, X.,&Yu, Z., 2015. Climate change and water
826 storage variability over an arid endorheic region. *Journal of Hydrology*, 529:
827 330-339.

-
- 828 Ye, S., Li, H.-Y., Li, S., Leung, L.R., Demissie, Y., Ran, Q., & Blöschl, G., 2015.
829 Vegetation regulation on streamflow intra-annual variability through adaption
830 to climate variations. *Geophysical Research Letters*, 42(23): 10307-10315.
- 831 Ye, S., Li, H.Y., Li, S., Leung, L.R., Demissie, Y., Ran, Q., & Blöschl, G., 2016.
832 Vegetation regulation on streamflow intra-annual variability through adaption
833 to climate variations. *Geophysical Research Letters*, 42(23): 10,307-10,315.
- 834 Yuan, W., Liu, S., Liu, H., Randerson, J.T., Yu, G., & Tieszen, L.L., 2010. Impacts of
835 precipitation seasonality and ecosystem types on evapotranspiration in the
836 Yukon River Basin, Alaska. *Water Resources Research*, 46: W02514.
- 837 Zeng, R., & Cai, X., 2015. Assessing the temporal variance of evapotranspiration
838 considering climate and catchment storage factors. *Advances in Water*
839 *Resources*, 79: 51-60.
- 840 Zeng, R., & Cai, X., 2016. Climatic and terrestrial storage control on
841 evapotranspiration temporal variability: Analysis of river basins around the
842 world. *Geophysical Research Letters*, 43(1): 185-195.
- 843 Zha, T., Barr, A.G., van der Kamp, G., Black, T.A., McCaughey, J.H., & Flanagan, L.B.,
844 2010. Interannual variation of evapotranspiration from forest and grassland
845 ecosystems in western canada in relation to drought. *Agricultural and Forest*
846 *Meteorology*, 150(11): 1476-1484.

847 Zhang, D., Cong, Z., Ni, G., Yang, D.,&Hu, S., 2015. Effects of snow ratio on annual
848 runoff within the Budyko framework. *Hydrology and Earth System Sciences*,
849 19(4): 1977-1992.

850 Zhang, D., Liu, X., Zhang, Q., Liang, K.,&Liu, C., 2016a. Investigation of factors
851 affecting intra-annual variability of evapotranspiration and streamflow under
852 different climate conditions. *Journal of Hydrology*, 543: 759-769.

853 [Zhang, D., Liu, X., Zhang, L., Zhang, Q., Gan, R.,&Li, X., 2020. Attribution of](#)
854 [Evapotranspiration Changes in Humid Regions of China from 1982 to 2016.](#)
855 [Journal of Geophysical Research-Atmospheres, 125\(13\): e2020JD032404.](#)

856 Zhang, L., Dawes, W.R. and Walker, G.R., 2001. Response of mean annual
857 evapotranspiration to vegetation changes at catchment scale. *Water Resources*
858 *Research*, 37(3): 701-708.

859 Zhang, S., Yang, H., Yang, D.,&Jayawardena, A.W., 2016b. Quantifying the effect of
860 vegetation change on the regional water balance within the Budyko framework.
861 *Geophysical Research Letters*, 43(3): 1140-1148.

862 Zhang, Y., Luo, Y., Sun, L., Liu, S., Chen, X.,&Wang, X., 2016c. Using glacier area
863 ratio to quantify effects of melt water on runoff. *Journal of Hydrology*, 538:
864 269-277.

865 Zhou, S., Yu, B., Huang, Y.,&Wang, G., 2015. The complementary relationship and
866 generation of the Budyko functions. *Geophysical Research Letters*, 42(6):
867 1781-1790.

868

869